AIAA-2000-3675

Development of a Micro-Isolation Valve: Minimum Energy Requirements, Repeatability of Actuation, and Preliminary Studies of Debris Generation

Juergen Mueller[1], Stephen Vargo[2], Amanda Green[3], David Bame[4], and Robert Orens[5]

Jet Propulsion Laboratory
California Institute of Technology
Pasadena, CA

Larry Roe[6]

Dept. of Mechanical Engineering
University of Arkansas
Fayetteville, AR

Continued experiments performed with a micro-isolation valve are being reported upon. This valve type is a microfabricated, silicon based device in which a doped silicon plug is being removed upon actuation with a capacitive discharge. Resistive heating melts and cracks the plug, opening the flow passage. This valve is for one-time use only, serving as an isolation valve in feed systems requiring zero-leakage sealing over long periods of time, such as future microspacecraft-based interplanetary missions, or advanced electric propulsion feed systems applications. In this study it was shown that valves could be actuated with capacitance as low as 0.6 μF using a 100 V charge. Required energies to melt the plug range into the tens of mJ for most cases, and valve actuation is fast, typically within the 0.1 – 0.3 msec. Valve repeatability, as determined by flow rate measurements after firing, range between 5 – 50% depending on operating conditions. Since plug breakage appears to be part of the valve actuation process, small particulates ranging in size around 1 micron or less are being generated that will require porous filter designs rather than previously contemplated microfabricated comb filter approaches to ensure trapping of these particles within the valve body.

I. INTRODUCTION

The advent of microspacecraft designs necessitates the development of novel, extremely miniaturized components. Within the propulsion area, attention has recently been focused on the development of microfabricated thrusters using so-called Microelectromechanical Systems (MEMS) technologies[1]. In order for such micropropulsion approaches to be sensible, however, other system components, such as valves, flow sensors and controllers, regulators, etc. will have to be miniaturized as well to similar degrees. Microvalves present extraordinary challenges in their miniaturization due to the fact that moving parts are present, and sufficient sealing forces will have to be generated within the small valve package at reasonable power levels[2]. Even if such developments may ultimately prove successful, any valve that is to be actuated repeatably will leak across its seat to some degree. In conventional propulsion systems, so called isolation valves, typically relying on pyrotechnic actuation, are therefore being used to seal the propulsion system and provide zero leak rates prior to their use. A miniaturized version of such a device may be of particular importance to microspacecraft. For example, microspacecraft may be used in mission scenarios where these craft are attached to larger spacecraft to serve as probes in order to perform more risky portions of a mission. Therefore, the microspacecraft may be inactive for long periods of the mission during which propellant leakage should be avoided, in particular also in view of the limited propellant supply of such a small craft. In addition to microspacecraft applications, a miniaturized isolation valve may also find applications in advanced electric propulsion feed systems, both miniature or conventionally sized. The typically low flow rates in these systems could likely still be controlled with a microvalve, thus leading to mass and volume savings.

In this paper continuing experiments performed on such a micro-isolation valve are being reported upon. A schematic of the isolation valve chip can be seen in Fig. 1.

[1]Advanced Propulsion Technology Group
[2]MEMS Group, Microdevices Laboratory
[3]Academic Part Time Student (USC), MEMS Group, Microdevices Laboratory
[4]Propulsion Flight Systems Group
[5]Measurement, Test and Engineering Support Section
[6]Associate Professor, Mechanical Engineering Dept.

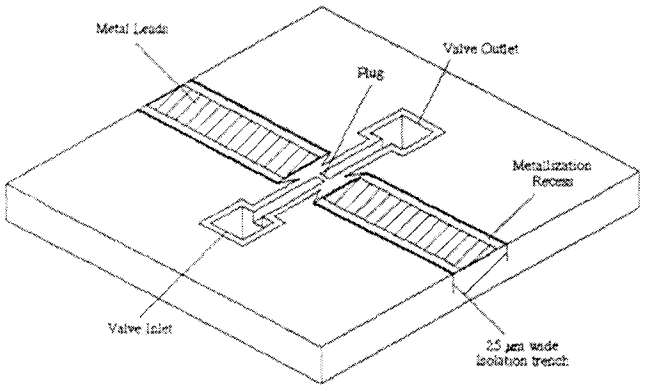

Fig. 1: The Micro-Isolation Valve Concept

The micro-isolation valve in its current form is a micromachined, silicon-based device that relies on the principle of melting a doped silicon plug, blocking the valve flow passage in the normally-closed position. A close-up of the channel passage and the sealing plug can be seen in Fig. 2. The plug is etched in place. Melting or cracking of the plug will open the valve and will be achieved by passing an electric current through the plug and resistively heating it. This current is being provided by a capacitive discharge. The valve will thus serve a similar function as a normally-closed pyrovalve, providing a zero leak rate prior to actuation by completely sealing the flow passage. Unlike a pyrovalve, however, the here proposed valve will not rely on pyrotechnic actuation, thus avoiding the potential for pyroshocks. It will also allow for ultra-compact valve integration with other MEMS-based propulsion components through integration on a chip, or chip-to-chip bonding.

In previous studies pressure handling capabilities of the valve were studied, and successful valve actuation was demonstrated for the first time[3,4]. In the present study, after giving a brief review of the valve design and results previously obtained with it, continued valve actuation experiments will be discussed. The goal of these experiments is to determine minimum valve driver capacitance (and thus minimum energies) required to open the valve. In addition, studies of valve actuation repeatability (from chip to chip) were conducted and preliminary findings will be reported upon. Finally, an initial examination of valve generated debris was performed. The latter issue represents an important feasibility criteria of the valve since debris generated by the plug due to the melting/breakage of the plug will have to be contained within the valve itself to avoid contamination of other flow components possibly located further downstream.

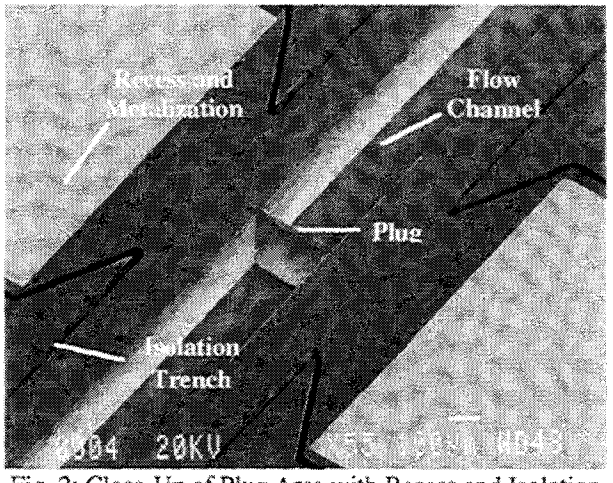

Fig. 2: Close-Up of Plug Area with Recess and Isolation Trench

II. THE MICRO-ISOLATION VALVE CONCEPT: PREVIOUS RESEARCH AND SCOPE OF CURRENT STUDY

Description of Concept

The micro-isolation valve concept has been described previously in Ref. 3. Briefly, the valve is silicon-based and fits on a chip 1 x 1 x 0.09 cm^3 in size. A photograph of a valve test chip is shown in Fig. 3. In this valve concept, flow is prevented from exiting the valve prior to actuation by a doped silicon barrier (or plug) blocking the flow. This plug is an integral part of the valve structure, machined by etching it into place, and does not feature any seals that may be compromised through contamination or vibrations experienced by the valve. To actuate the valve, an electric current is passed through the narrow plug (10 - 50 micron thick). As a result of the heat dissipation caused by the current passing through the plug, the plug melts or cracks partially and is blown away through the force of the upstream propellant pressure, thus opening the valve. All flow channels are etched into the silicon portion of the valve. A Pyrex wafer anodically bonded to the silicon wafer seals the flow channels from the top. A silicon-Pyrex anodic bond was chosen due to its superior strength, as well as the ability to view plug and flow channel through the Pyrex during experimental investigations of this valve.

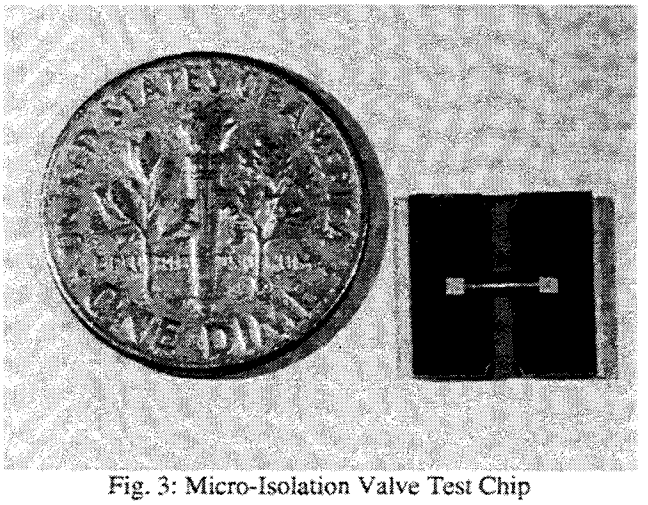

Fig. 3: Micro-Isolation Valve Test Chip

Previous Research

Several key feasibility issues need to be addressed in the development of this valve concept, such as (1) the demonstration of plug melting within acceptable energy levels; (2) acceptable pressure handling capabilities; and, (3) the demonstration of trapping of plug debris within the valve body to avoid contamination of other flow components downstream. Previous experiments were able to show that this type of valve is able to sustain pressures up to about 3,000 psig[3]. Two burst pressure failure modes were observed. In cases of plug thicknesses at or below 20 micron, plug failure was observed due to breakage. Typical burst pressures in the cases of 20-micron plugs were found to be around 2,500 psig. Above 20-micron plug thickness, Pyrex failure occurs, typically in the form of break-throughs in the Pyrex just above the valve inlet. Typical burst pressure values range between 2,500 psig to about 3,000 psig. The thicker plugs (25, 35, and 50 micron) remained intact at these pressure values. Pyrex thickness was 0.5 mm and it is expected that use of thicker Pyrex may further increase burst pressures.

In addition, valve actuation could be demonstrated successfully during previous studies. A limited number of chips featuring 25-, 35-, and 50-micron plugs were fired and opened. Energy levels required to open the plug were estimated to be in the range of 10 mJ for the thinner plugs (25-micron) and up to 120 mJ for the thicker (50-micron) plugs. A capacitive discharge was used to generate the required power levels. Capacitances used in these tests ranged between 6 and 30 μF. As a result of the capacitive discharge, very fast valve actuation was observed. Thinner plugs operated using smaller and faster discharging capacitances were estimated to open within 0.1 ms, while larger plugs using larger (slower discharging) capacitances opened within 0.7 ms or less.

Typically, for an isolation valve that will only be opened once at the beginning of the mission to activate the propulsion system actuation times are not critical from a systems perspective. However, in the case of the here considered silicon-based isolation valve fast actuation is crucial to limit heat losses from the plug into the remainder of the chip. Early studies had shown that too slow an actuation is unable to open the plug and, instead, leads to delamination between the silicon and Pyrex wafers. This is due to heat diffusion across the chip and differences in coefficient of thermal expansion (CTE) between the silicon and Pyrex used (Dow Corning 7740) at elevated temperatures (> 300 C) and the applied internal pressure.

Scope of Present Study

In the present study valve actuation is investigated further and in greater detail. In particular, emphasis is placed on actuation energies required to open the plug in order to reduce capacitor sizes. Reduction in capacitor sizes will have significant impacts on the overall system design. The reduction in capacitor size will also lead to still faster valve actuation, however, given the already fast response times noted previously, this was a side-effect and not the goal of the further study of this valve. In the course of this study some scatter in flow data through previously opened valves was observed, prompting a closer examination of valve repeatability (chip-to-chip) and preliminary findings of these studies will be presented. Finally, some early, and very preliminary, data on valve generated debris will be discussed.

III. DESCRIPTION OF EXPERIMENT

A series of valve actuation experiments was conducted. These tests consisted of firing numerous valve chips (approximately 120), recording voltage and current traces during valve actuation, calculating power values, calculating resistance traces and determining valve actuation times from these (see below), and calculating required energy levels to open the valve by integrating the power curve over the valve actuation time. After valve firing, the test chips were subjected to flow tests to evaluate repeatability of valve actuation, and a certain number of chips was imaged under a Scanning Electron Microscope (SEM) to obtain further clues regarding observed valve behavior. Various components of the experimental set-up are described in the following.

Valve Test Chips

The test chip design was alluded to in the previous section and is shown schematically in Fig. 1. The chip design focuses solely on the plug region and the optimization of the plug design, and, thus, does not yet contain any design features to trap plug debris, such as internal filters. The chip features a straight, 4 mm long channel section with a cross section of 300 x 300 μm^2. The plug is located in the center of the chip, dividing the channel section into two sections of equal length. Several different plug designs were tested, including 25-, 35-, 50-, and 100-μm plugs. The channel is connected to an inlet and outlet through which gas can enter and exit the chip.

The chip is sealed with an anodically bonded Pyrex cover. This seal necessitates the fabrication of two recesses into the chip which feature the electric leads connected to the plug, visible as the lightly-colored rectangular regions in Fig. 3. Since metal deposition may be as thick as several tenths of a micron, depositing the metal lead directly onto a non-recessed silicon surface would have led to leakage paths immediately adjacent to the metal deposits, as the Pyrex would have been forced to bend over them. Although doping of silicon is possible to provide electric contacts, its resistivity is higher than that of gold, and since the desire was to create the majority of the voltage drop in the plug region where heating was supposed to occur, gold was chosen as connecting material. The chip itself can be

electrically contacted near the edges, where notches in the Pyrex (see Fig. 3) are machined.

Wrapping around the recess area and the entire channel section is a narrow, 25-μm wide isolation trench. It can be seen in Fig. 2. This trench serves as an electrical insulation. Note that the entire top surface of the chip is doped to a depth of 4 micron. In order to ensure that most of the current flows through the plug and not around the channel section, a high resistivity path is created around the channel, constrained by the channel itself and the isolation trench. This path is about 200 μm in width over several millimeters in length. Extensive use of advanced deep trench reactive ion etching (RIE) techniques was made during chip fabrication leading to the desired vertical plug walls as shown in Fig. 2.

Valve Actuation Test Set-Up

The test chips were mounted onto a stainless steel fixture to provide connectors to the gas supply. Nitrogen gas was used in all experiments as the working fluid. Typically valves were fired at an upstream feed pressure of 300 psig, although some tests were performed at pressures as high as 1280 psig, and at pressure levels between these two values. The valve exit was exposed to ambient. The chip fixture bearing the chip was installed into a probe station where the chip could be contacted electrically via two probe tips, as seen in Fig. 4. The chip was connected via these probes and connecting leads to a capacitive discharge ignition circuitry (valve driver). This driver circuitry was modified from the one used in previous tests[3]. In order to test valves at lower driver capacitances, the capacitance internal to the ignition circuit was lowered from 4 μF to 0.6 μF. Additional capacitance could be installed external to the ignition circuitry and in parallel to the 0.6-μF internal capacitor, thus allowing driver capacitance to be varied throughout the tests. The capacitors where typically charged to 100V. This value was chosen since it resulted in a significantly less complex ignition circuitry design than would have been the case if high voltage had been used. However, future testing of this valve may be conducted with higher voltages, thus allowing the required capacitance to b reduced further.

Current and voltage traces were recorded on a storage scope (Tektronix TDS 744A) at sampling frequencies of typically 250 kHz, then transferred to a PC for processing. Voltage traces were read directly into the scope and current traces were recorded as voltage drops across a 0.095 Ω shunt internal to the driver circuit and later converted into current data using a simple Ohm's law approach. Similarly, power traces were calculated from recorded voltages and currents. The time dependent valve resistance, obtained by dividing the voltage trace by the current trace, was also calculated. A technique briefly alluded to in Ref. 3 was used to estimate valve response times. Inspection of the resistance traces showed that resistance increases rapidly during heating of the plug.

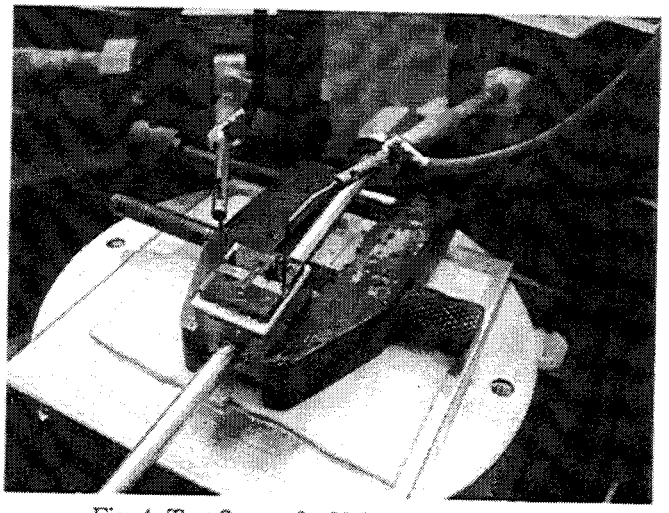

Fig. 4: Test Set-up for Valve Actuation Tests

Assuming that maximum heating and maximum resistance coincide with each other and are reached just prior to valve opening, the valve response time can be estimated. It was assumed to be the time elapsed between the onset of the voltage and current spikes and the point in time the maximum value of the resistance is reached, i.e. the point in time where the valve is assumed to open. This approach, its motivation and reasoning behind it, as well as assumptions made in its use, as well as its limitations in particular with respect to very fast valve actuation at low driver capacitance, are discussed in greater detail in the Appendix.

The energy required to open the valve was then determined by integrating the power trace over valve response time by means of a simple trapezoidal integration. Average power over this time interval was obtained by dividing the energy required to open the valve by the valve response time. Typically, three identical valves were fired under identical conditions to estimate data scatter.

Flow Test Set-Up

After actuation of the valves they were subjected to flow testing in order to study repeatability of valve actuation. The valves were connected to the same pressurant supply used in the valve actuation tests (nitrogen), with a nitrogen-calibrated flow meter (Sierra Model 500-sccm) installed into the line. Typically three feed pressure values were adjusted to obtain a short data curve for each of the three valve firings obtained under identical conditions.

IV. RESULTS OF VALVE ACTUATION TESTS

Approximately 120 isolation valves were tested in this study, featuring plug thicknesses of 25, 35, 50, and 100 micron. Data shown below are for the 25-, 35, and 50-micron cases only. Eight 100-micron chips were also tested, however, could not be opened even using a driver capacitance as high as 60 μF.

Voltage, current and calculated power traces for two chips (featuring a 25-micron and a 50-micron plug, respectively) are shown in Figs. 5-7 and are representative of other chips as well. Notice the very sharp voltage, current and power spikes for the 25-micron chip, which is due to the use of a very small driver capacitance of merely 0.6 μF, discharging much more rapidly than the larger 7.6 μF capacitor used with the 50-micron chip. Peak voltage values typically range around 60-80 V, peak current values reach as high as 8 A, and power values typically peak between 500 – 750 W.

While these numbers appear high, notice that due to the fast capacitor discharge, energy values provided to the chip are quite low. Figure 8 shows energy values calculated suing the aforementioned procedure for 25-, 35-, and 50-micron plugs fired using various capacitances. Note that energies are displayed in milli-Joule in the figure. Energy levels are as low as 3 mJ in the case of a rapidly fired 25-micron plug, and reach as high as 60 mJ in the case of a 50-micron plug using a large, 17-μF driver capacitance. These energy values appear very compatible with microspacecraft applications.

As expected, thicker plugs require more energy to open, and thus demand larger capacitance to actuate. These larger capacitances further increase energy demands to cause plug melting as can be seen when inspecting Fig. 8. Clearly, for the same plug larger capacitances result in higher energy demands for the same size plug to open. This may be explained by the fact that larger capacitors discharge more slowly, which may lead to higher heat conduction losses into the remainder of the chip. In fact, in early testing it was noted that too slow a valve actuation would lead to excessive heating of the entire chip, causing delamination between the silicon and Pyrex wafer due to CTE differences, while leaving the plug itself intact.

Figure 9 shows the estimated valve response time, i.e the time elapsed between triggering the capacitor discharge and the actual valve opening. As alluded to above, and further detailed in the Appendix, these valve actuation times were estimated from calculated resistance traces, which in turn were derived from the recorded voltage and current traces using Ohm's law. Using this approach, one arrives at valve actuation times of approximately 0.3 – 0.4 ms in high-capacitance 50-micron plug cases to as little as 0.1 ms or less in the case of 25-micron plugs fired at 0.6 μF capacitance.

Inspecting Figs. 8 and 9, two important further observations can be made. In Fig. 8, the energy traces for the 25- and 35-micron plugs seem to be increasingly non-linear at very low capacitance values, and seem to be larger than a purely linear energy-capacitance relationship would suggest. This effect is small and may just be due to scatter

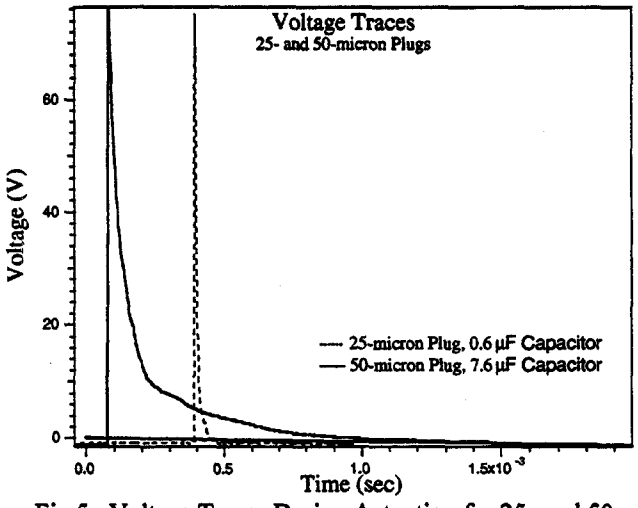

Fig 5.: Voltage Traces During Actuation for 25- and 50-micron Plugs

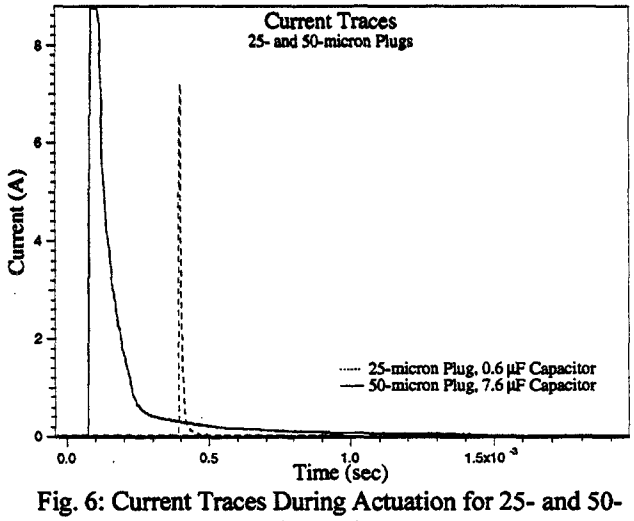

Fig. 6: Current Traces During Actuation for 25- and 50-micron Plugs

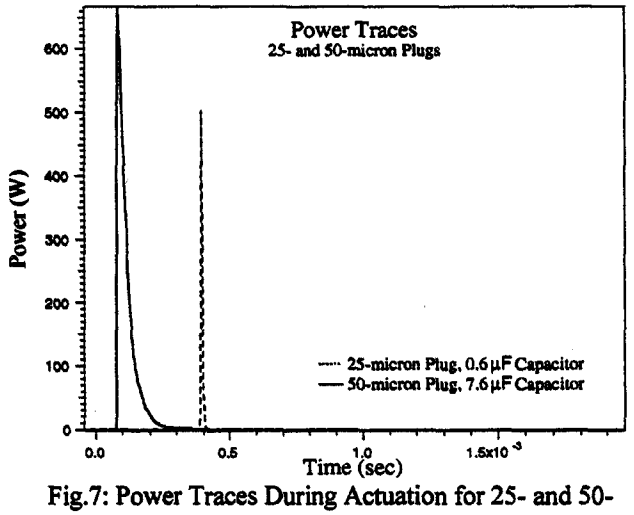

Fig.7: Power Traces During Actuation for 25- and 50-micron Plugs

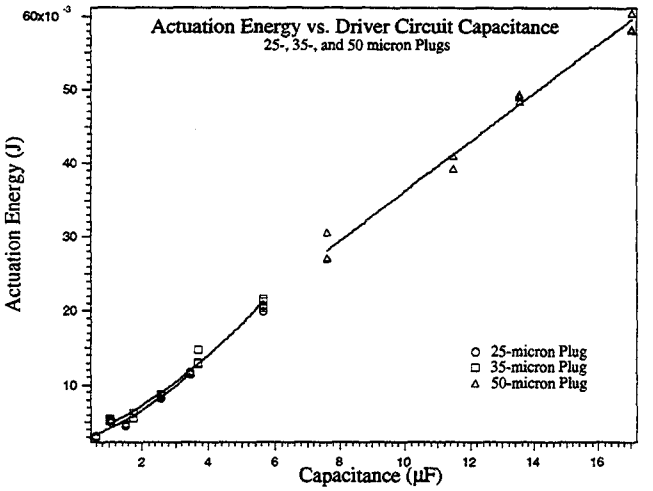

Fig. 8: Actuation Energy vs. Driver Circuit Capacitance for Various Plug Sizes

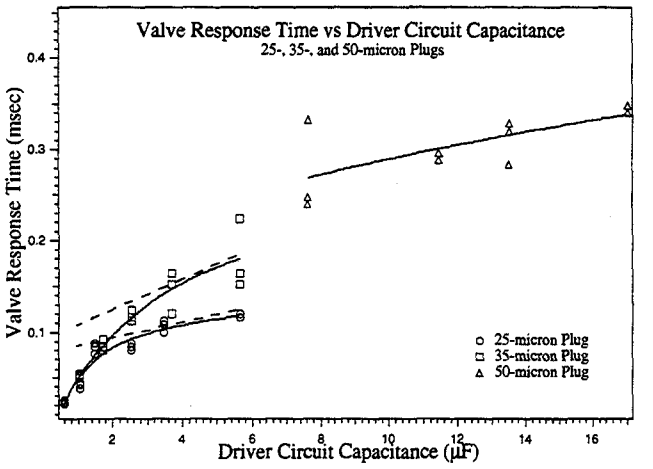

Fig. 9: Valve Response Times vs. Firing Circuit Capacitance for Various Plug Sizes

in the data. On the other hand, it may be a real effect. As valve firings become shorter due to faster-discharging, smaller capacitors, heat losses into the chip structure eventually will become negligible, and the required energy value may asymptote to the amount of energy actually required to cause plug melting.

Secondly, inspecting Fig. 9, response times seem to decrease steeply as capacitance is lowered below 3 μF or so in the case of 25- and 35-micron plugs. However, as is noted in the Appendix, the approach used to estimate the valve response time may underestimate time values for very fast valve actuations using very small capacitance. It is currently believed that the steep decrease in response times is at least partially due to the failure of the resistance trace approach detailed in the Appendix to accurately determine valve response times accurately for these low capacitances. According to the Appendix, actual response times may be larger for very low capacitance by up to a factor of two. However, erros associated with this method appear significantly less pronounced at higher capacitances, such as in the 50-micron cases, possibly amounting to 10 % or less.

Using the response times determined for the larger capacitances of the 25- and 35-micron curves, as well as the linear relationship of response time versus capacitance for the 50-micron plug as a guide, higher response times may actually result as illustrated by the dashed lines. Note that these dashed lines are not meant to indicate actual data, but merely serve to indicate a trend in data that may have been present if errors associated with the determination of very short response times had been smaller. As a consequence, calculated actuation energy values in these cases would also increase, and the aforementioned effect of asymptoting energy values for low capacitances may become more pronounced. Future, alternate approaches of determining valve response times, as outlined in the Appendix, may yield a more accurate picture.

A key goal of these experiments was the determination of the minimum capacitance required to open the valve. Reducing required capacitances to actuate the valve will result in smaller, lighter weight ignition circuitry, easier integration between valve and this circuitry, and more compact system designs. Results of these tests show that only in the case of the 50-micron chips did the plug fail to open below a given capacitance, namely 7.6 μF, representing the left-most points on the 50-micron curve of Fig. 8 and 9. Using the next lowest capacitance of 5.66 μF failed to open the chip as could be verified by flow tests performed after chip firing (see next section). Therefore, minimum required capacitance at a 100 V charge is somewhere between these two capacitance values for a 50-micron plug. The minimum energy value determined in this case was approximately 27 mJ.

The thinner 25- and 35-micron plugs opened in all cases, even for the lowest capacitance of 0.6 μF, representing the internal capacitance of the valve driver unit. In the case of 35-micron plugs, the valve barely opened in these cases, indicating that minimum capacitances may be near 0.6 μF for a 100 V charge, corresponding to energy values of about 5 mJ. As mentioned above, at these low capacitances, energy levels may have been underestimated (see Appendix). No limit was found for the 25-micron plugs, only in a few cases reported further below did the plug barely open at 0.6 μF.

It should be noted that even smaller capacitance values could be afforded if capacitors could be charged to higher voltages. In space applications, one practical concern of such an approach would be the generation of such high voltages onboard a microspacecraft without significant mass penalties. At present, a 2-cm^3 power conditioning module weighing 4.25 grams and providing voltages in the range between 0-± 5000 V is commercially available[5]. Output power, however, is limited to a maximum of 1.25 W at

present. However, given that each micro-isolation valve will only be fired once during the course of the mission, the driver capacitance can be charged over considerably longer time periods than the typical valve response time. This in turn will lower required power values far below those generated during valve actuation.

Given the range of capacitors tested with 50-micron plugs, it was deemed worthwhile to examine these plugs under the electron microscope to study potential differences in plug removal. Results are shown in Figs. 10 through 15. Since the Pyrex cover is opaque to electrons, it had to be removed in order to view the opened barrier. Brightly colored regions in the figures are remnants of this Pyrex cover and not germane to the discussion. In each case, the chip serial number is noted inside the figure. Figures 10 and 11 show 50-micron plugs fired at 3.5 μF and 5.7 μF capacitance, respectively, i.e. below the minimum capacitance required to open the valve. As can be seen when inspecting these two figures, damage, apparently due to plug melting, can only be detected near the top edges of the plug. The center section of the barrier remained intact and bonded to the Pyrex cover, providing no leakage path. It is believed that the concentration of damage near the plug edges is due to the skin effect, i.e. the fact that a highly transient electric current flows near the surface of a conductor. Obviously, during a capacitive discharge the electric current is highly transient as indicated in Fig. 6, for example. For the lower capacitance case shown in Fig. 10, these current transients are even more pronounced since the smaller, 3.5 μF capacitor discharges more rapidly then the 5.7 μF capacitor used with the chip shown in Fig. 11. Therefore, the skin effect is more pronounced as well and damage is more concentrated near the edges of the plug, as can be seen when comparing Figs 10 and 11 closely.

It is interesting to note in either Fig. 10 or 11 how this damaged region fans out beyond the plug location onto the surface of the chip. These "rays" had been observed previously[3]. At that time, with the Pyrex cover still mounted to the silicon chip, it was not certain whether the damage had actually occurred within the silicon or the Pyrex, and cracking of the Pyrex had actually been suspected as being responsible for the pattern observed. In fact, as Figs 10 and 11 show, this damage is part of the silicon surface. Since the damaged regions located beyond the plug and those located near the plug edge interconnect and show the same surface dislocations, it may be reasoned that they are due to the same high currents flowing along the plug edges. They may in fact represent transition regions where the skin-effect dominated current through the plug fans out as it continues on towards the much wider (2 mm width) gold leads.

As capacitance is increased, more energy is channeled into the plug, and current transients slow. The skin effect is reduced and combined with the larger energy deposition into the plug the entire top surface of the plug is now being melted, opening a leakage path across the top of the barrier. Evidence of melting is quite visible in Fig. 12, showing the case of a 50-micron plug fired with a 7.6 μF capacitor. This case represents the onset of valve opening, i.e. one of the left-most data points in the 50-micron curve of Figs. 8 and 9.

Further increase in capacitance (and thus energy deposited into the plug) removes ever larger sections of the plug. In Fig. 13, showing the case of a 50-micron plug fired with an 11.5 μF capacitor, plug melting is still very evident. Interestingly, cavities form near the edges of the barrier where the plug connects with the channel walls. This effect has been noticed repeatedly and at present is not understood. One explanation suggests that these may not be due to melting at all but, rather, due to high thermal stresses were the heated plug connects to the cooler bulk of the chip.

Increasing the driver capacitance even further results in even wider valve openings, with no clear difference noticeable anymore between the cases of a 13.6 and a 17.1 μF drive capacitor. However, noteworthy is the different appearance of the opened plug in both cases (see Figs 14 and 15) when compared to the previous figures. Closer inspection of the top surface of the plug remnant reveals sharp ridges, and no longer any smoothly contoured edges as in the case of lower-capacitance valve firings. This seems to indicate that in these cases the valve may have opened due to cracking. The following explanation is being offered to explain this observation: As the valve firing is initiated, the top of the plug, featuring a 4 micron deep doped layer, is resistively heated and likely molten as in lower capacitance cases. However, the larger amount of energy deposited into the plug due to the use of a larger capacitance causes larger sections of the plug to heat up, although possibly not quite to melting temperatures. The still rapid heating process (valve response times are 0.3 ms or less in these cases, see Fig. 9!) may cause steep thermal gradients to develop even within the high-thermal conductivity silicon plug material, causing thermally induced stresses, which in turn may lead to cracking and subsequent breakage of the barrier. As will be shown below, initial studies of debris generated during valve firings does indeed indicate particle generation due to melting *and* fracture, indicating that both processes occur during the valve actuation process. A slightly different picture emerges for thinner plugs, as will be discussed in the next section.

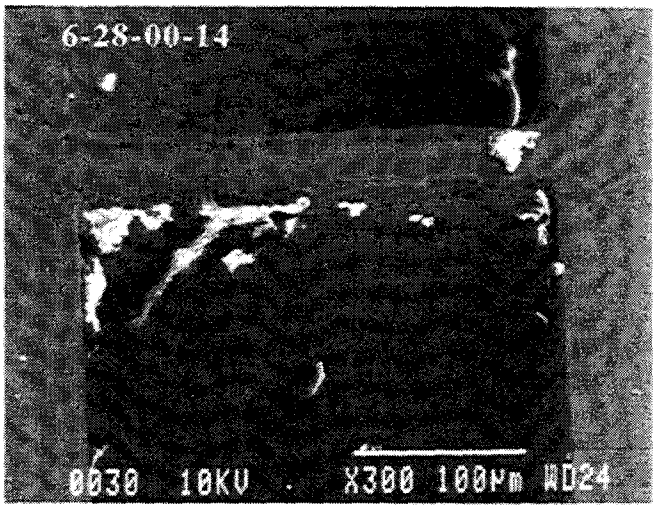

Fig.10: 50-micron Plug, 3.5-µF Capacitance

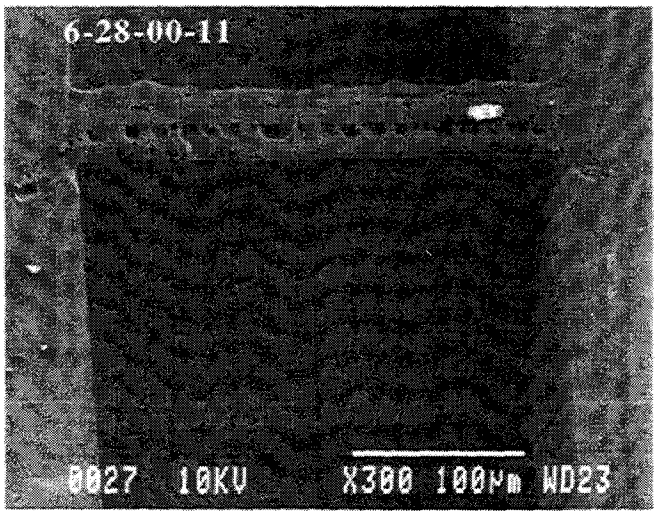

Fig.11: 50-micron Plug, 5.7-µF Capacitance

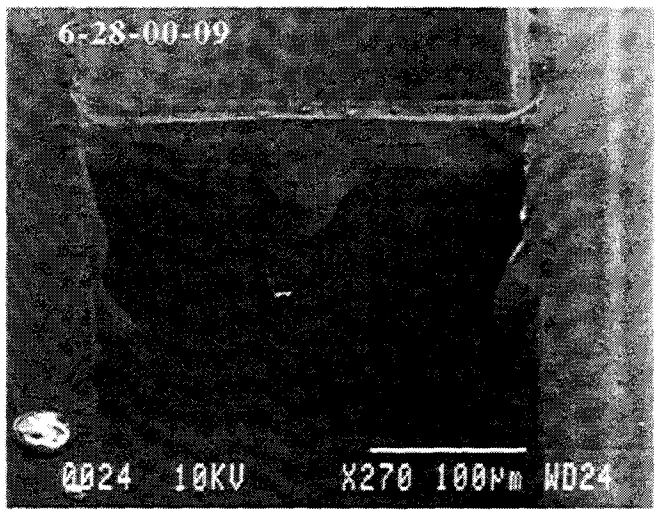

Fig.12: 50-micron Plug, 7.6-µF Capacitance

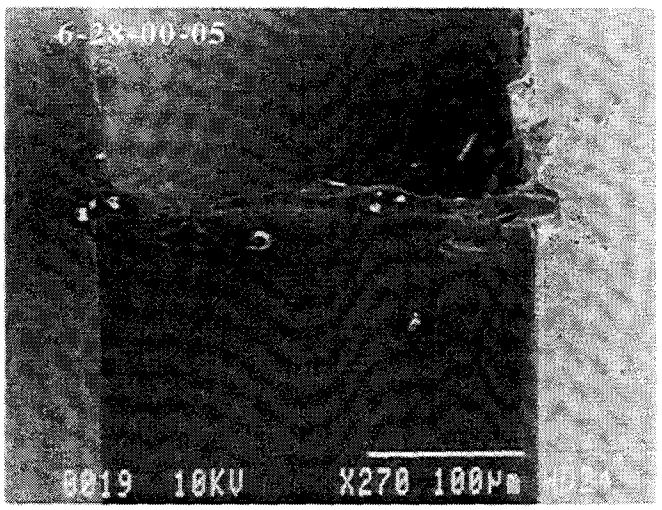

Fig.13: 50-micron Plug, 11.5-µF Capacitance

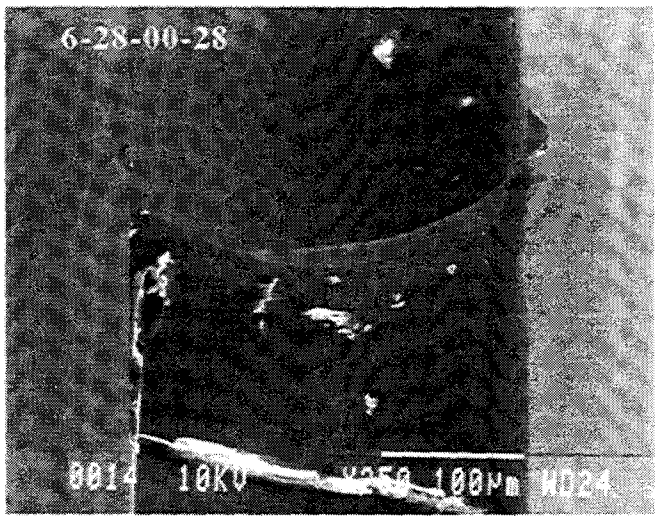

Fig.14: 50-micron Plug, 13.6-µF Capacitance

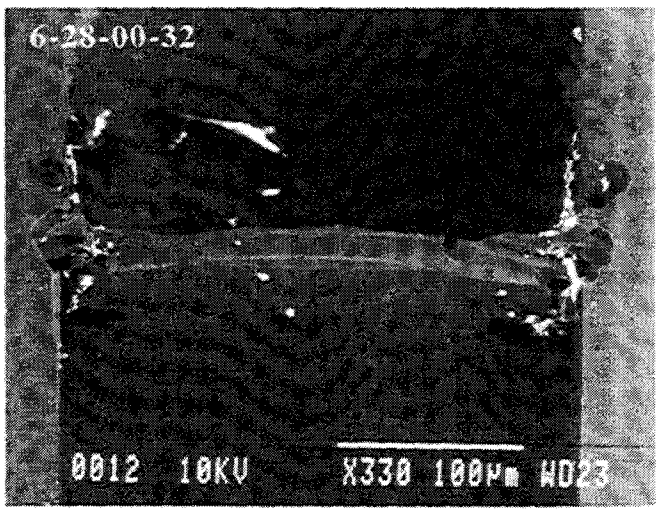

Fig.15: 50-micron Plug, 17.1-µF Capacitance

V. RESULTS OF VALVE REPEATABILITY TESTS

Following valve firings, valves were subjected to flow tests in order to determine the repeatability of valve actuation. To this end, in most cases at least three valves of the same type were tested under identical conditions with respect to capacitance and feed pressure to allow for comparisons. In a few cases, fewer chips were available. It is being realized that a larger statistical sample of chips is required to obtain more accurate data regarding valve repeatability. However, note that every chip may only be fired once, and numerous operating conditions were studied, limiting the number of chips available to test one particular operating condition.

Results of flow tests conducted with various plugs are shown in Figs 16 through 18. In each figure, triplets or doublets of curves are shown, each representing a set of flow tests performed for a given plug width and capacitance used in the valve firing. The curves were generated by applying a feed pressure to the valve inlet, and measuring the flow rate through the valve for three or four different pressures. Pressures were read off gages located several feet upstream of the valve. Thus, actual inlet pressures at the valve may have been slightly lower. Pressures could be read within 0.1psi increments on a 30 psi scale, 0.25 psi increments on a 100 psi scale, and 2.5 psi increments on a 1500 psi scale, representing approximately the error associated with pressure readings. The flow meter (Sierra Model 500-sccm) was calibrated prior to use and flow readings were taken with accuracies of about 1 sccm. Typically, flow rates were taken several minutes after a certain feed pressure had been adjusted to allow the flow and meter to stabilize.

Figure 16 shows the case of 50-micron plugs. The scatter in flow data for the lower capacitances (7.6 and 11.5 μF) can clearly be seen and are high, in some cases approaching 50% of the highest flow rate measured. Noteworthy, however, is the considerably smaller scatter in flow data for higher capacitances (17.1 μF) being no larger than 10%. Similar results were obtained for a pair of chips fired at 13.6 μF (not shown in Fig 16). Obviously, this result deserved further study to determine whether the observed lower scatter in flow rate data in these cases is coincidental or a real effect. Unfortunately, four additional 50-micron chips that were available for testing all leaked around the perimeter of their bond interface with the chip fixture. Flow rate measurements for these operating conditions will therefore have to be delayed to a future point in time when new 50-micron chips become available.

Similar curves plotted in Fig. 17 for 35-micron plugs indicate a similar flow behavior, with the exception of one curve for a 5-μF firing resulting in significantly lower flow rates. A similar large scatter of data can be found for 25-micron plugs, as shown in Fig. 18. Here only one triplet of curves is shown due to this large scatter of data.

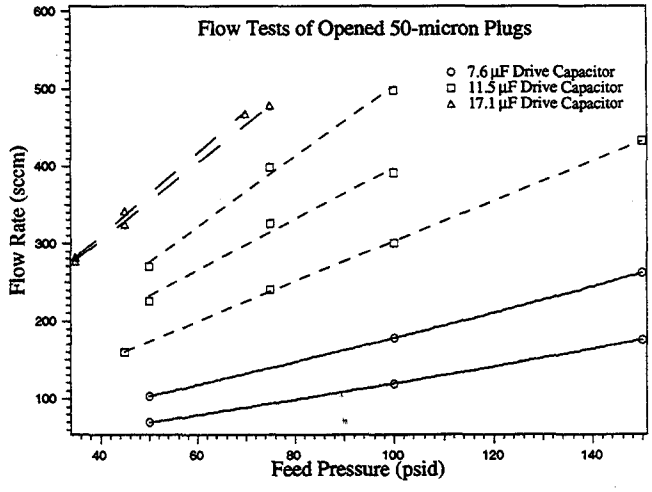

Fig. 16:Measured Nitrogen Flow Rates Through Opened 50-micron Plugs

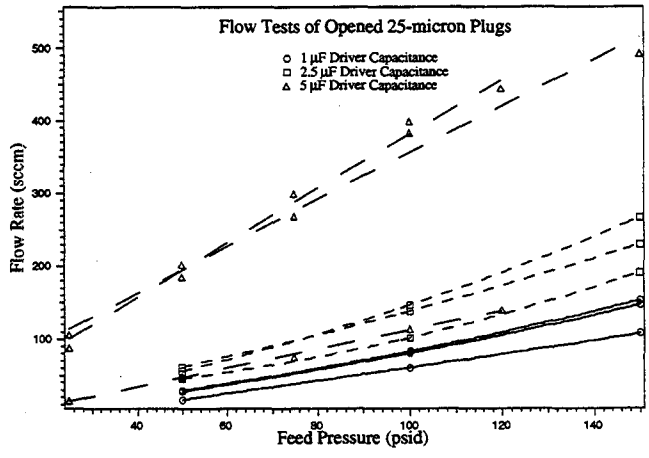

Fig. 17: Measured Nitrogen Flow Rates Through Opened 35-micron Plugs

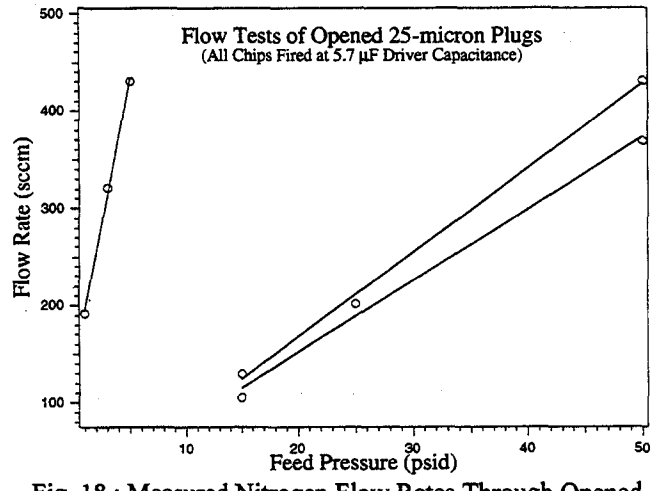

Fig. 18 : Measured Nitrogen Flow Rates Through Opened 25-micron Plugs Fired at Intermediate Pressures (300 psid) and High Capacitance (5.7 μF)

However, the case shown in Fig. 18 is typical for all triplets of 25-micron chips tested. In each case, one of the three chips tested under identical conditions sustained significantly higher flows.

Inspection of these valve chips under an electron microscope provided an explanation for this behavior. Figures 19 and 20 show two of the three 25-micron chips for which flow data have been displayed in Fig. 18. As can be seen, plug opening differs strongly in the two cases. Noteworthy is the pronounced degree of fracture as shown in Fig. 19 when compared to 50-micron cases displayed earlier. This tendency of the thinner plugs to fracture more easily may explain the large scatter of flow data, recognizing the relative randomness of fractures.

Figure 20 shows the high-flow case of Fig. 18. As can be seen, the entire plug has been removed. If this type of plug removal could be triggered in a controlled fashion, good valve actuation repeatability should result given that the valve opening is now largely determined by the channel cross sectional area, and would thus be relatively predictable. It was suspected that operating thinner plugs at elevated pressures may cause this type of plug opening to occur more frequently. Figure 21 shows a series of flow tests performed with 25-micron chips that had been fired at an elevated feed pressure of 750 psig. As can indeed be seen, all cases show a high-flow behavior similar to the single high-flow case shown in Fig. 18, indicating that the same type of plug removal as shown in Fig. 20 had occurred in all three valve firings at 750 psid.

Examination under the SEM of these three plugs fired under the higher pressure conditions shows indeed a better repeatability of valve openings, as can be seen in Figs 22 through 24. Large sections of the plug have been removed in all cases, although some larger sections of the plug near the corners of the flow channel remained in place. These obstructions, and their irregular shape as a consequence of the fracture process, may have contributed to the remaining scatter in the flow data measured for these plugs. This remaining scatter in flow data, however, has been reduced to approximately 20% in the worst cases using this approach as can be seen by inspecting Fig. 21. Note also the debris located in the flow channels of these cases. This debris appears to have been molten and appears to be sticking to the channel wall surfaces. This seems to indicate that even in these cases of valve openings where plug fracture appears to dominate, plug melting is still occuring.

The test was repeated for lower driver capacitance of 0.6 and 2.9 μF capacitance. The case of the 0.6-μF firing is shown in Fig. 25. Although high-flow cases (likely similar to the one shown in Fig. 20) were triggered in two cases, one of the valves fired barely opened. Therefore, repeatability of valve actuation may require a combination of thin plugs, high pressurization, and sufficient energy to trigger the plug removal process. It should be noted,

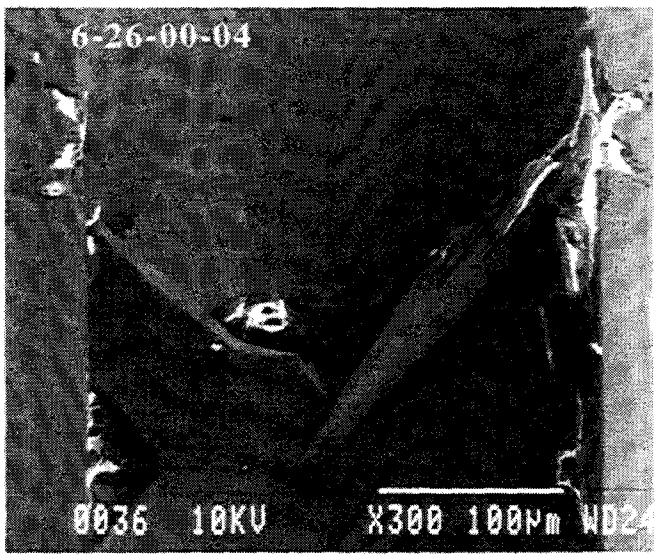

Fig. 19: 25-micron Plug, 5 μF Capacitance

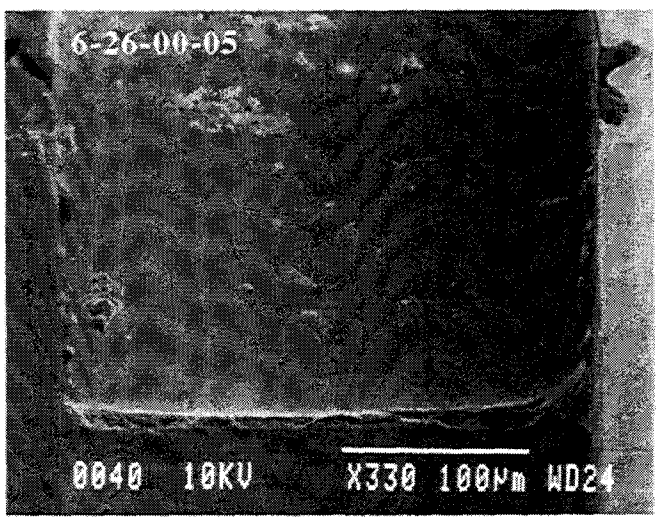

Fig. 20: 25-micron Plug, 5 μF Capacitance

however, that these findings are highly preliminary at this point. Using the data obtained in this study, however, more targeted future investigations can now be performed. For example, a study of plugs featuring vertical notches etched into them may result in better predictability of fracture patterns and valve actuations.

VI. INITIAL VALVE DEBRIS STUDIES

Initial studies of valve debris generation were performed. As was mentioned in Sect. II, debris generation due to plug opening is a major feasibility issue for the micro-isolation valve. Debris generated by the valve during the actuation process must not be allowed to contaminate any flow components than may be located downstream of the valve. Proper filtration of any debris generated is essential. In order to determine appropriate filter designs, the amount and type of (size distribution of

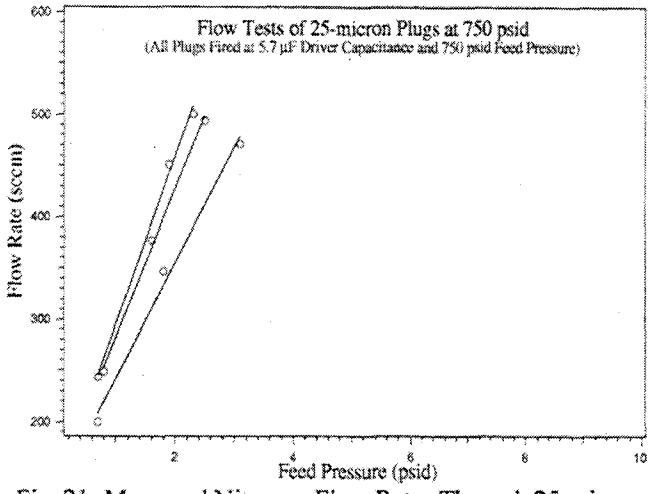

Fig. 21: Measured Nitrogen Flow Rates Through 25-micron Plugs Fired at 750 psid Pressure and 6.2 µF Capacitance

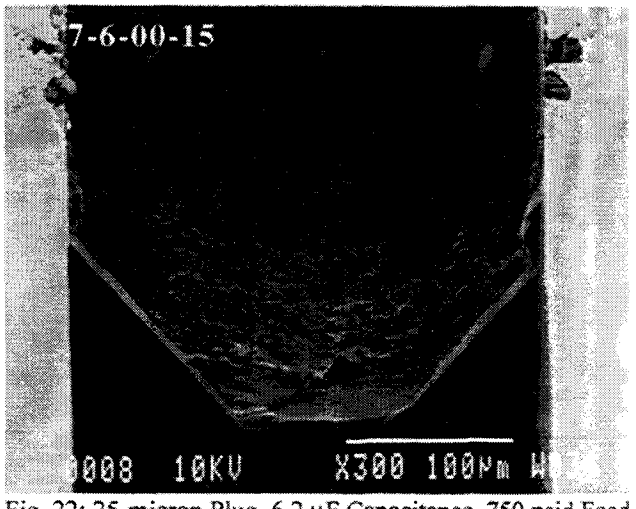

Fig. 22: 25-micron Plug, 6.2 µF Capacitance, 750 psid Feed Pressure

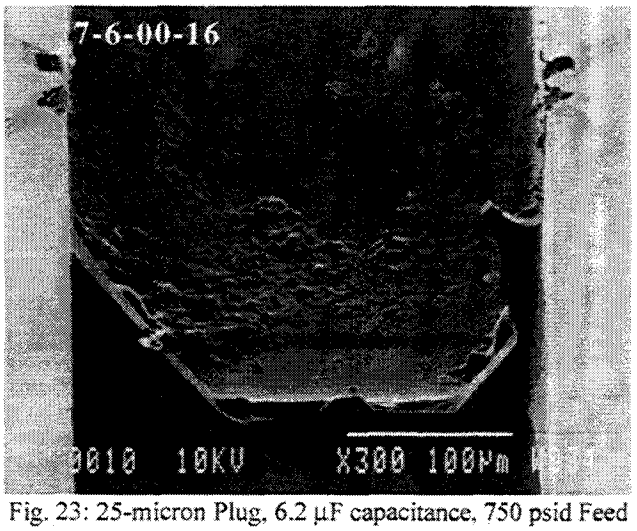

Fig. 23: 25-micron Plug, 6.2 µF capacitance, 750 psid Feed Pressure

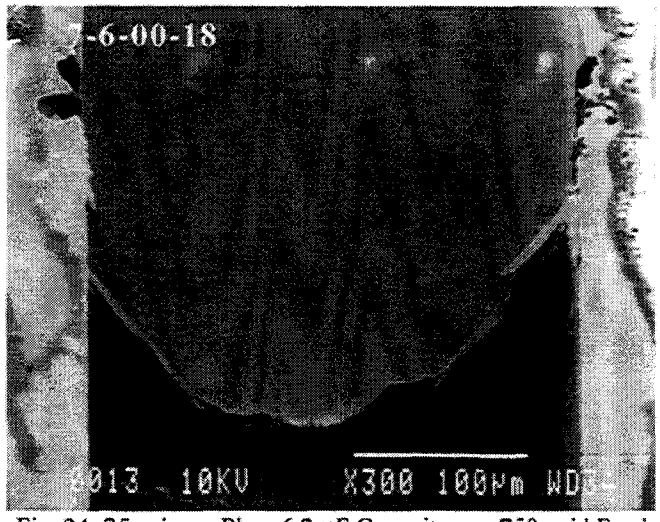

Fig. 24: 25-micron Plug, 6.2 µF Capacitance, 750 psid Feed Pressure

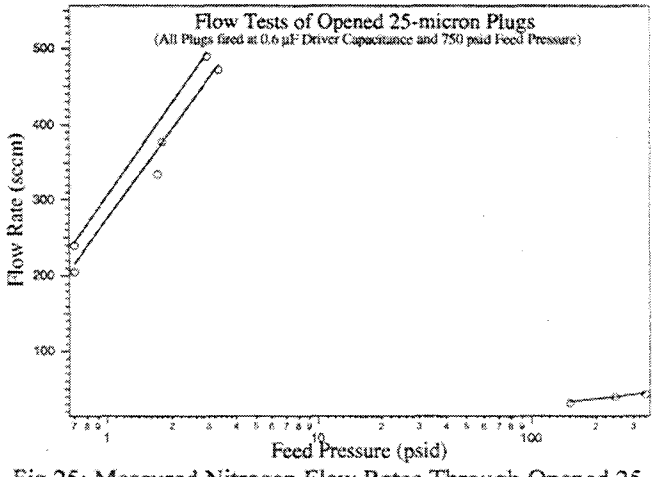

Fig.25: Measured Nitrogen Flow Rates Through Opened 25-micron Plugs Fired at Elevated Pressures (750 psid) and Low Capacitance (0.6µF)

particulates) has to be known first. A test series to characterize valve-generated debris with the goal of designing proper filtration schemes has recently been initiated. At present, only very preliminary findings were obtained, and activities in this area of valve research are anticipated to be stepped up significantly in the future to address this third and final of the major valve feasibility issues.

A 25- and two 35-micron chips were tested in this first experiment. These chips were mounted on a modified Plexiglas fixture, eliminating the outlet tube of the previously used stainless steel fixtures (compare with Fig. 4). Instead, the fixture allowed debris generated during the valve opening process to be directed into a sealed container featuring a filter pad, located immediately below the valve fixture. The transparent fixture and container allowed

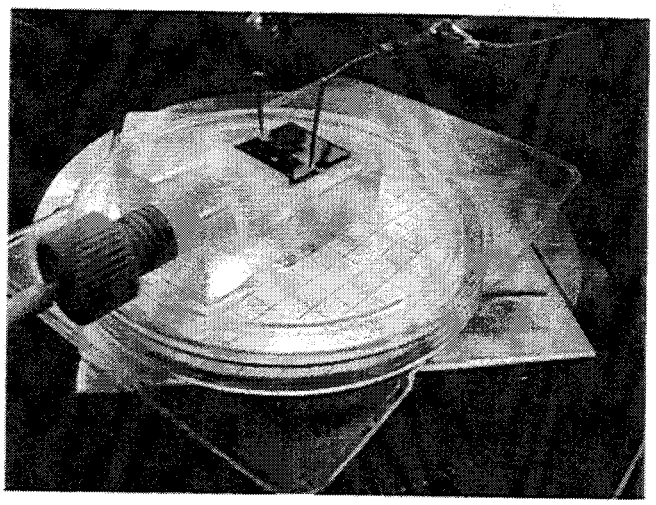

Fig.26: Chip Mounting for Debris Tests

viewing of the inside of the flow channel to determine if any debris may have located itself along the channel walls rather than being deposited onto the filter pad. After valve firing, the valve fixture with the valve chip can be replaced by a cover lid under controlled conditions, and the now sealed filter pad can be placed under a microscope or possibly an SEM for analysis. Typically, particles of given size ranges are counted for each square featured on the filter pad.

In these preliminary tests only qualitative examinations of the valve debris generated were conducted to date to be followed up by more time-consuming, thorough studies at a later date. Initial findings were that particulates found ranged in size as large as 10 micron and less than 1 micron in diameter. The latter were found most frequently. Both particulates appearing to have previously been molten (indicated by rounded surface features) as well as particulates likely resulting from plug fractures (as indicated by jagged edges and surfaces) were found. This finding appears reasonable in light of the plug opening mechanisms discussed above, involving both melting and fracture. As may be suspected, the smallest particulates (1 micron or less) typically feature jagged edges and irregular surfaces, indicating that these may have been generated during plug fracture processes.

These smaller particles will be most difficult to trap. Since they have not previously been molten, they cannot be condensed on cold surfaces, as was previously observed to have occurred for some plug debris (see Ref. 3). Similarly, previously discussed comb filter approaches[3] may not be sufficient to filter this small-scale debris. Such comb filters, consisting of a series of silicon posts etched into place inside flow passages, may not be able to be fabricated with small enough filter ratings (post spacings) to trap sub-micron debris. At sub-micron length scales, lithography may place limitations on fabrication of such filters. Using even the most advanced deep trench reactive ion etching (RIE) techniques, aspect ratio limitations also have to be taken into account. Typically, vertical features with aspect ratios of less than 30 can be machined, meaning that for a 1 micron filter post spacings posts can only be machined to a height of 30 microns. This would result into extremely shallow and wide flow passages. Wider flow passages, however, will result in larger areas of the chip to be pressurized, and reduce the available bond area accordingly thus either limiting the pressure handling capability of the chip, or increasing its overall size (see Ref. 3).

At present it appears that comb filter approaches may still be required in order to trap large debris as shown in Fig. 19. Additional, molten debris generated in the valve actuation process may be condensed on special traps, however, small sub-micron particles resulting from plug fractures may have to be filtered using other means. Unfortunately, at present, valve fracture, such as the type shown in Fig. 20, appears to show the highest degree of valve repeatability, and may have to be relied upon for that reason in the future, requiring novel filtration approaches to be explored. At present, the insertion of conventionally machined and commercially available porous filter plugs into the isolation valve chip is being considered as a near-term solution, rendering the micro-isolation valve concept a MEMS-hybrid. Other, more radical MEMS-based approaches are currently being brainstormed as well. In either case, it is anticipated that a significant amount of future work will be devoted to this area.

VII. CONCLUSIONS

Continued studies of a micro-isolation valve were reported upon. Based on earlier experiments, which demonstrated the ability of the valve to open using capacitive discharges, further valve actuation experiments were conducted. Several new, important findings were obtained:

(1) Valves can be actuated with capacitances as low as 0.6 μF and less in the case of 25- and 35- micron plugs, and require a minimum capacitance of 7.6 μF in the case of 50-micon plugs for a 100 V capacitor charge. Corresponding minimum energies required to open the valve are estimated to be around 27 mJ in this latter case, with valve actuation times being around 0.25 ms.

(2) Capacitance could be reduced further if higher voltage charging could be provided. Presently available small high-voltage drivers are about 2 cm^3 in size, weigh about 0.5 gram and are able to provide up to 5 kV voltage at about 1 W, allowing for a slow high-voltage capacitor charge.

(3) Valve opening is thought to take place as a result of melting and cracking of the plug. Initially, the doped top layer of the plug is molten during the applied power pulse. Thermal shock of the remainder of the plug due to rapid heating of the top sections leads to the

will be discussed below). It was argued that the time elapsed between the discharge trigger and this peak (indicated by the two vertical lines in Fig. A1) is the time period during which plug melting/opening occurs, corresponding in in this case to a time period of approximately 0.3 ms.

The reasoning behind this argument is that as the plug heats, and possibly portions of it are being removed, the resistance of the plug material and thus the valve should increase. Maximum resistance should be reached at the time of valve opening when heating is greatest and the valve opens, disrupting the current path. Obviously, resistance decreases again after the peak, which initially was thought to be due to cooling of the valve. However, a series of experiments, to be described below, determined this decrease in resistance to be an artifact of the computation of the resistance curve. As the capacitor discharges and ever smaller voltages are divided by ever smaller currents, this calculation eventually gives erroneous results. An indication of this is given in the left of Fig. A1 at a time prior to triggering the discharge. Here voltage and current are at their respective noise levels and the calculated resistance is an artificial number. Actual pre-test resistance in this case was 10.8 Ω and post test resistance was 26.78 Ω measured using an Ohm Meter both before and after the test.

To confirm the reasoning given above for the isolation valve test, a 25-Ω non-inductive resistor was tested using the same driver circuit, however, using a 20-μF capacitor. Voltage and current values were recorded as for the valve tests using a storage scope, and resistance traces calculated from these data. As can be seen in Fig. A2, the calculated resistance rises to a level just below 25 Ω, then slowly decreases as for the 50-micron plug in Fig. A1. Very noticeably, the broad peak at the beginning of the curve noticed for the valve and associated with the plug melting process, is missing. Furthermore, the calculated resistance trace does not reach the 25-Ω value measured under steady state conditions. This may be due to the fact that the resistance curve decreases as a result of the discharging capacitor as described above.

Next, a 10-Ω, 0.125-A fuse was subjected to the same test, using a 20-μF capacitive discharge as well as in the case of the 25-Ω non-inductive resistor. Results are shown in Fig. A3. Notice that in this case the resistance increases gradually at first, as in the case of the broad peak region of the 50-micron plug trace shown in Fig. A1, then enters a singularity. The singularity is due to the fact that as the fuse opens, the current drops to zero (or, rather, its noise level) and the calculated resistance trace diverges.

Obviously, there are some similarities between the valve plug and a fuse, and noticing similar behavior for both was encouraging. To more closely simulate the isolation valve, however, the same type of fuse was now placed in parallel to the 25-Ω non-inductive resistor (Fig. A4). Thus, as the fuse opens, current can continue to flow through the

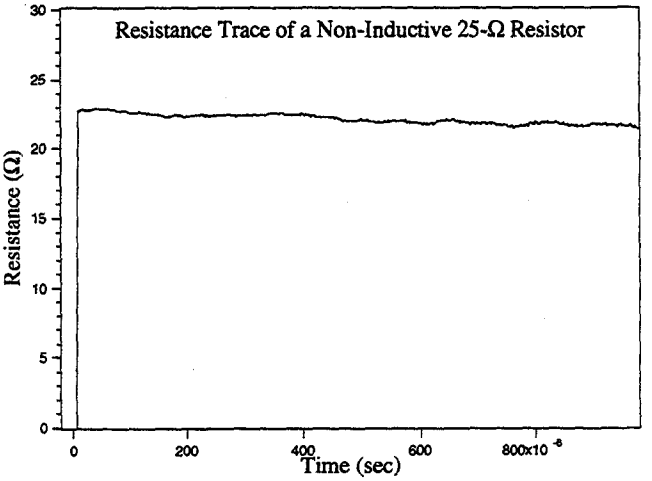

Fig.A2: Resistance Trace of a Non-Inductive 25-Ω Resistor

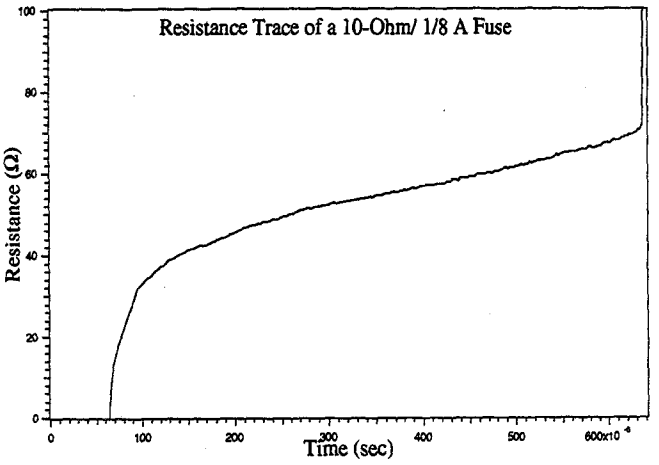

Fig. A3: Resistance Trace of a 10-Ω/ 0.125-A Fuse

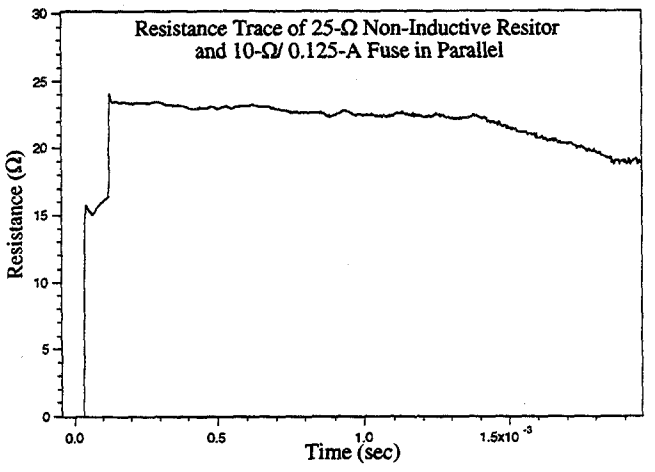

Fig. A4: Resistance Trace of 25-Ω Non-Inductive Resistor and 10-Ω 0.125-A Fuse Switched in Parallel

development of thermal stresses and cracking of the plug.

(4) Thinner plugs are much more prone to cracking than thicker plugs in the process described under Item (3), as may be suspected. This results in poorer valve repeatability for these thinner plugs, unless operating conditions are carefully selected.

(5) Operating thinner plugs at higher pressures and sufficiently large driver capacitance in order to deposit the necessary energy to induce thermal shock, 25-micron plugs were shown to be able to open almost completely, i.e. resulting in the removal of the virtually the entire plug. This approach may be selected to achieve greater valve repeatability in the future. Using this approach, measured scatter in flow rate data between same-type valves fired under identical conditions could be reduced to 20% or less, down from 50% or more in other cases.

(6) Valve repeatability may be improved further if notches are etched into the plug, triggering predictable cracking at those locations.

(7) Relying on plug breakage to enhance valve repeatability will increase challenges to filter design. Plug breakage appears to generate very small (1 micron or less in diameter) particulates that are difficult to trap using micromachined comb filter approaches. Porous plug filters, to be integrated with the valve, may offer a near-term solution but would render the valve a MEMS-hybrid. Other MEMS-based porous filter approaches are currently being contemplated.

VIII. ACKNOWLEDGMENTS

The authors greatfully acknowledge the support of Mr. Frank Razo in assembling the data acquisition system used in these tests.

The research described in this paper was carried out at Jet Propulsion Laboratory, California Institute of Technology, under a contract with the National Aeronautics and Space Administration.

IX. REFERENCES

[1]Mueller, J., "Thruster Options for Microspacecraft: A Review and Evaluation of State-of-the-Art and Emerging Technologies", to be published in "Micropropulsion for Small Spacecraft", edited by Micci, M. and Ketsdever, A., AIAA Progress Series, Vol. 187, 2000.

[2]Mueller, J., "A Review and Applicability Assessment of MEMS-Based Microvalve Technologies for Microspacecraft Propulsion", AIAA Paper 99-2725, 35th Joint Propulsion Conference, Los Angeles, CA, June 20-24, 1999.

[3]Mueller, J., Vargo, S., Bame, D., Fitzgerald, D., and Tang, W., "Proof-of-Concept Demonstration of a Micro-Isolation Valve", AIAA Paper 99-2726, 35th Joint Propulsion Conference, Los Angeles, CA, June 20-24, 1999.

[4]Mueller, J., Vargo, S., Chakraborty, I., Forgrave, J., Bame, D., and Tang, W., "The Micro-Isolation Valve: Introduction of Concept and Preliminary Results", AIAA Paper 98-3811, 34th Joint Propulsion Conference, Cleveland, OH, July 13-15, 1998.

[5]EMCO High Voltage Corp., Company Information.

APPENDIX

In the evaluation of the micro-isolation valve the valve response, or valve actuation, time, i.e. the time elapsed between the point in time when the ignition circuit is triggered to the point the plug removal process is complete and the valve is actually open, is a useful parameter. It allows the power trace to be integrated over this time period and thus provides information regarding how much energy is actually needed to open the plug. Note that the total energy stored in a capacitor will actually be higher as the capacitor will continue to discharge through leakage paths around the plug at low voltage and current levels after valve opening.

Initially, pressure sensors located into the flow path downstream of the valve were to be used to measure the pressure pulse after valve opening and allow the valve response time to be determined. However, difficulties arose during the set-up of these sensors, to be elaborated upon further below. While performing the tests, however, interesting features were noted in the resistance trace of the valve during the valve actuation process. This resistance curve was generated by dividing voltage and current traces using Ohm's law. A typical trace is shown in Fig. A 1 for a 50-micron plug fired at 17.1 μF capacitance. Note the broad resistance peak soon after triggering the discharge. (The smaller, initial spike is believed to be due to induction in the long leads connecting the ignition circuit to the valve, as

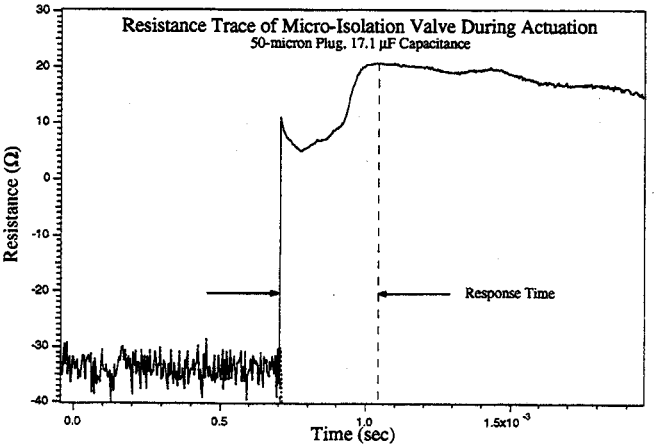

Fig. A1: Resistance Trace of a 50-micron Plug During Valve Actuation (17.1 μF Capacitance)

resistor, as current continues to flow through surrounding regions of the plug in the valve after firing. The obtained trace now very closely resembles in shape that obtained with the 50-micron plug and by analogy it was reasoned that the broad peak in the resistance trace is indeed due to plug melting, allowing valve actuation times to be estimated.

Note also a small spike immediately flowing the trigger of the discharge in Fig. A4. This spike, as mentioned previously, was noticed also in the 50-micron plug trace. Through another set of experiments it was determined that it was caused by the long leads connecting the valve driver circuit to the valve (or the simulated resistor/fuse assembly, respectively) and possibly due to inductive resistance building up in the leads. Shortening the leads in another resistor/fuse test eliminated this peak.

This approach thus may present a quick, easy and cheap-to-implement way to estimate valve response times, and actuation energies through integration of the power trace over the valve response period. In the current research environment of demanding and ever tightening schedule and cost requirements, this approach has obvious benefits. However, there appear to be limitations to this approach for very fast valve actuations, as is demonstrated in Fig. A5. As was noted earlier, the calculated resistance traces do not appear to reach their true peak value, which is believed to be due to the non-steady capacitive discharge. As voltage and current values drop, calculated resistance values become increasingly erroneous. As in Fig. A1, the effect of this can be seen to both the far left and right of the trace in Fig. A5, representing the resistance values calculated using noise data. The decrease in resistance therefor appears to be a transition to these noise data.

The actual value of the calculated resistance during the valve opening process is of little importance in this approach since the peak is merely used as a marker in time, regardless of its size. However, it is possible that the peak is also being shifted to the left in this process. For the valve of Fig. A5, the post test resistance value measured under steady state conditions was 26.65 Ω. If one were to extrapolate the initial incline of the resistance trace to this value, as indicated by the dashed line in Fig. A5, a crude estimate regarding the shift of this peak to the left of Fig. A5 results. As indicated by the dashed lines, the resulting valve actuation times may be increased by between 50-100 % in this case.

The case depicted in Fig. A5 is admittingly the most extreme found during this set of experiments. Using the same approach for the 50-micron plug trace of Fig. A1, errors much smaller (10% or less) result. Obviously, these estimates do not represent a strict error calculation and merely give an indication of the limitations of this approach as actuation times become very fast. Errors of this approach could be judged more accurately if independent ways of measuring valve actuation times were implemented. As mentioned above, one such approach may be the use of

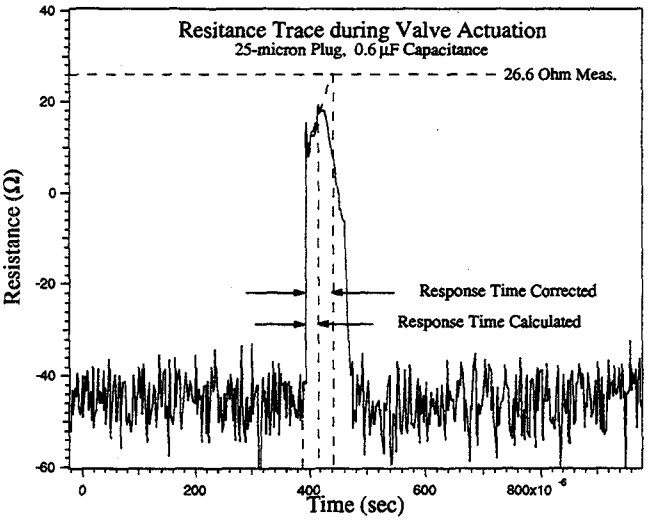

Fig. A5: Resistance Trace of a 25-micron Plug During Valve Actuation (0.6 µF Capacitance)

pressure sensors placed into the flow path downstream of the valve. Note, however, that valve actuation is so fast, that delays due to the final velocity of the pressure pulse travelling from the plug to the location of the sensor will have to be taken into account and may lead to errors in the measurements as well. It may be conceivable to use two pressure sensors mounted a known distance apart. The time elapsed between the pulses arriving at the two sensors would allow the velocity of the pressure pulse to be measured. Using this measured velocity, a correction may be derived in order to account for the delay of the pulse arriving at the first sensor due to the finite distance this pulse has to travel between plug and this sensor. This approach obviously bears within it the assumption of constant speed of sound along the entire flow path, which may or may not be true, depending on how different temperature and pressure conditions are near the plug when compared with those at the pressure sensor locations.

This error could be reduced further if microfabricated sensors were to be used, mounted directly into the downstream flow path of the chip. Fabrication of such chips, however, may be considerably more complicated and costly, and at present no such chips have been built. Should the accurate determination of the very fast valve actuation times for very low-capacitance valve actuation be considered crucial to the evaluation of the feasibility of this valve, such an approach may be implemented in the future.